Lung (2015) 193:619–627
DOI 10.1007/s00408-015-9750-6

STATE OF THE ART REVIEW

Tuberous Sclerosis Complex: State-of-the-Art Review with a Focus on Pulmonary Involvement

Felipe Mussi von Ranke[1] · Gláucia Zanetti[1] · Jorge Luiz Pereira e Silva[2] · Cesar Augusto Araujo Neto[2] · Myrna C. B. Godoy[3] · Carolina A. Souza[4] · Alexandre Dias Mançano[5] · Arthur Soares Souza Jr.[6] · Dante Luiz Escuissato[7] · Bruno Hochhegger[8] · Edson Marchiori[1]

Received: 21 March 2015 / Accepted: 15 June 2015 / Published online: 24 June 2015

Abstract Tuberous sclerosis complex (TSC) is an autosomal-dominant neurocutaneous disease with high phenotypic variability. The incidence is approximately one in 5000–10,000 births. TSC is characterized by widespread hamartomas and benign or rarely malignant neoplasms affecting various organs, most commonly the brain, skin, retinas, kidneys, heart, and lungs. The wide range of organs affected reflects the roles of TSC1 and TSC2 genes in the regulation of cell proliferation and differentiation. Clinical diagnostic criteria are important because genetic testing does not identify the mutation in up to 25 % of patients. Imaging is pivotal, as it allows a presumptive diagnosis of TSC and definition of the extent of the disease. Common manifestations of TSC include cortical tubers, subependymal nodules, white matter abnormalities, retinal abnormalities, cardiac rhabdomyoma, lymphangioleiomyomatosis (LAM), renal angiomyolipoma, and skin lesions. Pulmonary involvement consists of LAM and, less commonly, multifocal micronodular pneumocyte hyperplasia (MMPH), which causes cystic and nodular diseases, respectively. Recent reports indicate that pulmonary LAM is found by computed tomography in up to 35 % of the female patients with TSC. MMPH is rare and may be associated with LAM or, less frequently, occurs as an isolated pulmonary manifestation in women with TSC. Dyspnea and pneumothorax are common clinical presentations of LAM, whereas MMPH is usually asymptomatic. The aim of this review is to describe the main clinical, imaging, and pathological aspects of TSC, with a focus on pulmonary involvement.

Keywords Tuberous sclerosis complex · Imaging · Computed tomography · Lymphangioleiomyomatosis · Lung diseases

✉ Edson Marchiori
edmarchiori@gmail.com

1 Federal University of Rio de Janeiro, Rua Thomaz Cameron, 438. Valparaiso, Petrópolis, Rio de Janeiro CEP 25685.120, Brazil

2 Federal University of Bahia, Salvador, Brazil

3 M. D. Anderson Cancer Center, University of Texas, Houston, TX, USA

4 Ottawa Hospital Research Institute, University of Ottawa, Ottawa, Canada

5 Radiologia Anchieta, Anchieta Hospital, Taguatinga, DF, Brazil

6 Medical School of Rio Preto and Ultra X, São José do Rio Preto, SP, Brazil

7 Federal University of Parana, Curitiba, Brazil

8 Santa Casa de Porto Alegre, Porto Alegre, Rio Grande do Sul, Brazil

Introduction

Tuberous sclerosis complex (TSC) is a genetically determined multisystem neurocutaneous syndrome characterized by a classic clinical triad of facial adenoma sebaceum, epilepsy, and mental retardation [1–4]. TSC is the second most common phakomatosis, after neurofibromatosis type 1, and is the result of dysfunctions in cell differentiation, proliferation, and migration in the early stages of fetal development [1, 3]. The organs most commonly involved are the brain, skin, kidneys, lungs, retinas, and heart [2]. The earliest symptoms of TSC consist of heart tumors and cortical tubers, which can be seen prenatally. Classic manifestations such as cortical tubers or subependymal nodules, white matter (WM) abnormalities, retinal abnormalities, cardiac rhabdomyoma, lymphangioleiomyomatosis (LAM),

and renal angiomyolipoma (AML) allow a presumptive diagnosis, particularly when skin lesions are present [5].

TSC exhibits autosomal-dominant inheritance, with a reported incidence of one in 5000–10,000 births [6]. Penetrance is approximately 95 %, but clinical manifestations vary from minor to severe disease and only 7–37 % of patients have positive family histories [7, 8]. Extensive linkage analysis of families with TSC revealed that the syndrome is heterogeneous and localizable to gene mutations in two distinct chromosomes: TSC1 (chromosome 9q34) and TSC2 (chromosome 16p13), tumor suppressor genes that facilitate the production of hamartin and tuberin, respectively [7]. Mutated genes lead to abnormal control of cell growth, resulting in tumor formation throughout the body. Although recent advances in treatment have improved morbidity, the prognosis remains quite poor and nearly 40 % of patients die by the age of 35 years [5]. Demonstration of a pathogenic mutation in TSC1 or TSC2 in normal tissue is considered sufficient for the diagnosis of TSC, independent of clinical manifestations [9]. However, clinical diagnostic criteria are important because genetic testing does not identify the mutation in up to 25 % of patients [10]. The clinical diagnosis of TSC is based on the presence of at least two major or one major and two minor criteria (Table 1) [9]. Imaging plays an important adjuvant role in suggesting or confirming the diagnosis of TSC, as well as defining the extent of disease involvement. The aim of this review is to describe the clinical, imaging, and pathological manifestations of TSC, with a focus on pulmonary involvement.

Table 1 Diagnostic criteria for tuberous sclerosis complex [7, 11]

Major features
Hypomelanotic macule
Facial angiofibromas
Ungual fibromas
Shagreen patch
Retinal hamartomas
Cortical tuber
Subependymal nodules
Subependymal giant cell astrocytoma
Cardiac rhabdomyoma
Lymphangioleiomyomatosis
Renal angiomyolipomas
Minor features
"Confetti-like" skin lesions
Dental enamel pits
Intraoral fibromas
Retinal achromic patch
Multiple renal cysts
Nonrenal hamartomas
Cerebral white matter radial migration lines

Definite diagnosis: two major features or one major feature and two or more minor features. Probable diagnosis: one major and one minor feature. Possible diagnosis: one major or two or more minor features

Pulmonary Manifestations

Lymphangioleiomyomatosis

LAM is a rare disorder characterized by abnormal proliferation of smooth muscle cells (LAM cells). LAM often occurs in patients with TSC (TSC–LAM), but it may occur in a rare sporadic form (S-LAM) that affects the lungs, lymphatics of the thorax, and retroperitoneum, as well as the kidneys [11]. S-LAM is associated with mutations in the TSC2 gene and is considered a forme fruste of TSC [12]. It affects almost exclusively women of child-bearing age. TSC-LAM occurs in patients with germline mutations in TSC1 or TSC2. TSC-LAM, but not S-LAM, has been reported in males [12]. The reported prevalence of LAM in patients with TSC is 1–3 % [7], but it may be much higher (up to 35 %) in women with TSC [13]. TSC–LAM is approximately five times more common than S-LAM [14]. The average age at diagnosis of LAM is 35 years, with the risk increasing by about 8 % per year [12]. In both forms, the disease is characterized by diffuse interstitial proliferation of bundles of smooth muscle cells and cystic changes in the pulmonary parenchyma. Microscopically, smooth muscle-like cells (LAM cells) are present as clusters of immature spindle cells that stain with smooth muscle actin, progesterone receptor, and the melanocytic marker HMB-45 [15].

The hallmark feature of LAM is the presence of diffuse, well-circumscribed, thin-walled lung cysts [14, 16]. Clinically, LAM is characterized by progressive dyspnea on exertion, recurrent pneumothoraces, abdominal and thoracic lymphadenopathy, and abdominal tumors, including AMLs and lymphangiomyomas. Renal AMLs occur in approximately 80 % of patients with TSC, in contrast to 60 % of patients with S-LAM [12]. Hemoptysis with small amounts of blood is common in pulmonary LAM [15]. Pulmonary function tests usually show obstruction and less often demonstrate a restrictive pattern [15].

The diagnosis of LAM is based on characteristic computed tomography (CT) findings in addition to any one of the following: radiological and/or pathological diagnosis of renal AML, chylothorax or chylous ascites, pathological diagnosis of lymphangioleiomyoma, lymph node involvement by LAM, and a diagnosis of TSC [15]. Vascular endothelial growth factor-D, a lymphangiogenic factor, has been found to have high sensitivity and specificity for the diagnosis of LAM [15]. The European Respiratory Society guidelines recommend high-resolution computed tomography (HRCT) examination for all female patients with TSC at

18 years of age and, if normal, at 30–40 years of age. Patients with TSC and unexplained respiratory symptoms should be screened by HRCT, regardless of age [13].

The clinical course of pulmonary LAM is usually slow and progressive, ultimately leading to respiratory failure. The 10-year survival rate was estimated to be 79 % in a study involving 69 patients [17], and the presence of TSC did not affect survival. The median age at death in this series was 48 years. In another study, the estimated 10-year transplant-free survival rate was 86 % [18].

Classic features of LAM on HCRT allow a presumptive diagnosis and can obviate lung biopsy. They include thin-walled (<3 mm thickness) rounded cysts spread uniformly throughout the lungs (Fig. 1) [19]. The intervening lung parenchyma is usually normal, although reticular opacities are occasionally seen, likely reflecting interstitial edema due to lymphatic obstruction [20]. Communication between cysts and small airways is indicated by a decrease in cyst size on expiratory CT acquisitions [20]. Pneumothorax and chylous pleural effusion are the two major complications of pulmonary LAM (Fig. 2). Pneumothorax is seen at presentation in 39–53 % of patients and during the course of the disease in 60–81 % of patients. The risk of recurrent pneumothorax in LAM is greater than 70 % [13]. Chylothorax is less common, seen at presentation in up to 14 % of cases and after diagnosis in 22–39 % of patients [21].

LAM is considered to be a low-grade metastasizing neoplasm, and the metastatic potential is supported by the presence of circulating LAM cells found in blood, urine, chylous effusion, bronchoalveolar lavage fluid, and lymphatic

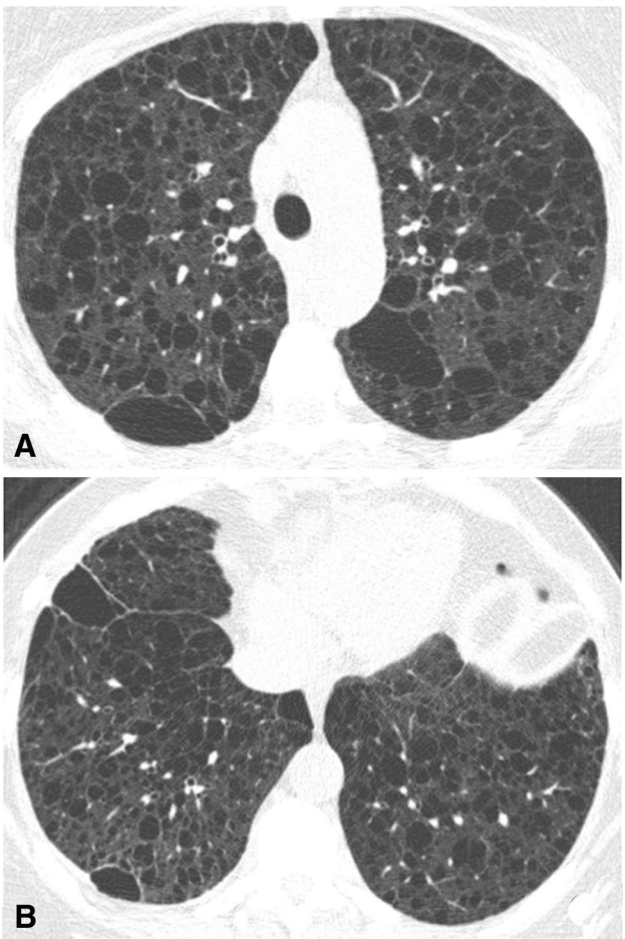

Fig. 1 A 42-year-old woman with tuberous sclerosis complex lymphangioleiomyomatosis. Axial CT images with lung window settings at the levels of the *upper* (**a**) and *lower* (**b**) lung regions show innumerable thin-walled cysts distributed uniformly throughout the lungs

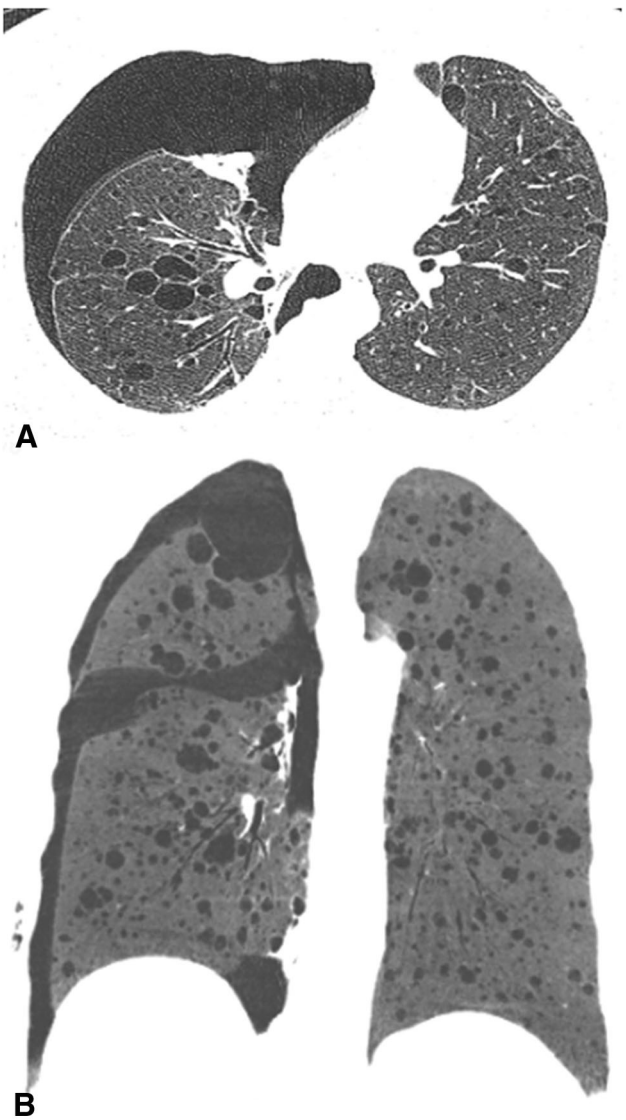

Fig. 2 A 52-year-old woman with sudden onset of right chest pain and dyspnea. Axial CT image with lung window settings (**a**) and coronal reformatted mini–maximum intensity projection image (**b**) show numerous bilateral, variably sized, thin-walled cysts (some subpleural), compatible with lymphangioleiomyomatosis and right-sided pneumothorax

systems of affected patients [22]. In the World Health Organization classification, LAM is listed as a mesenchymal tumor in the malignant epithelial tumor category [23].

The differential diagnosis of LAM on HRCT includes other cystic diseases, such as pulmonary Langerhans' cell histiocytosis (PLCH), Birt–Hogg–Dubé syndrome (BHDS), and lymphoid interstitial pneumonia (LIP) [15, 24–27]. In PLCH, cysts are variably sized and often have thickened walls and bizarre shapes. In contrast to LAM, cysts predominate in the upper and middle lung zones, sparing the costophrenic angles. The presence of nodules in the intervening lung is very suggestive of PLCH [15, 24]. Importantly, however, multiple fine nodules may be seen in TSC–LAM with multifocal micronodular pneumocyte hyperplasia (MMPH). In BHDS, thin-walled cysts, often larger, are distributed asymmetrically and predominate in the subpleural and paramediastinal regions of the lower lung zones. LIP typically manifests with few cysts and interstitial changes, such as reticulonodular and ground-glass opacities. Pneumothorax is more commonly seen in LAM than in BHDS and PLCH (reported in 10–25 % of cases), and may occasionally be the presenting manifestation of these diseases [24, 28]. Skin and kidney involvement is frequently seen in TSC–LAM and BHDS. In contrast to TSC, in which tumors are usually benign, BHDS carries an increased risk of renal cell carcinoma (RCC) [15, 24].

Multifocal Micronodularpneumocyte Hyperplasia

MMPH is the second most frequent pulmonary manifestation in TSC. It is a rare disorder characterized by multicentric, well-demarcated, nodular proliferation of type II pneumocytes along the alveolar septa [29, 30]. The absence of immunohistochemical staining for HMB-45 suggests a different histogenesis from pulmonary lesions in LAM [30]. MMPH has been reported in men and women with TSC and TSC-LAM, as well as in women with S-LAM [12]. Clinical manifestations include dyspnea, cough, and mild to moderate hypoxemia. Unlike LAM, MMPH is indolent and not progressive [29]. MMPH is characterized on HRCT by multiple solid nodules or nodular ground-glass opacities ranging in size from 2 to 10 mm, scattered throughout the lungs in a random distribution (Fig. 3). Although differentiation between MMPH and miliary metastatic or granulomatous disease may be difficult, MMPH should be considered in patients with TSC [12].

Other Thoracic Manifestations

Rare thoracic involvements in TSC include LAM involvement of the mediastinum or thoracic duct, and aortic or pulmonary artery aneurysm [31].

Fig. 3 A 46-year-old man with tuberous sclerosis complex. Axial CT image with lung window settings shows small nodular ground-glass opacities in both lungs. The histopathological diagnosis was multifocal micronodular pneumocyte hyperplasia

Neurological Manifestations

Neurological complications, including seizures and intellectual disability, are the major causes of morbidity in patients with TSC [32]. Epilepsy is the most common, affecting 80–90 % of patients [32]. Seizures often manifest in the first year (usually in the early months) of life [2]. Approximately 30 % of children with TSC have severely to profoundly impaired intellectual capacity. In addition to learning disability, autism spectrum disorders, attentional deficits, and other neurobehavioral abnormalities may occur [2].

Cortical Tubers

Cortical tubers are benign hamartomas of the cerebral cortex, thought to be the result of abnormal cellular differentiation and migration [33]. They are present in 95 % of patients with TSC and are closely related to the neurological manifestations of this complex [33]. Although 95 % of cortical tubers are multiple, solitary tubers are seen in rare instances [34]. Magnetic resonance imaging (MRI) is superior to CT for the detection and characterization of cortical tubers. They typically appear as well-circumscribed areas of low signal intensity on T1-weighted and high signal intensity on T2-weighted sequences [35] (Fig. 4b).

Subependymal Nodules

Subependymal nodules are another common form of hamartomatous lesion in patients with TSC. They can occur anywhere along the ventricular surface, but are most commonly found in the caudothalamic groove near the foramen of Monro [36]. CT is useful for the detection of subependymal nodules because they commonly (88 %)

demonstrate calcification when compared with cortical tubers [35]. On MRI, they show intermediate signal intensity on T1-weighted images and isointense to hyperintense signals on T2-weighted images [35].

Subependymal Giant Cell Astrocytomas

Subependymal giant cell astrocytomas (SEGAs) are lesions derived from subependymal nodules, usually a gradual process occurring in the first two decades of life. The prognosis is generally good, as SEGAs grow slowly, rarely invade the brain, and infrequently undergo hemorrhage or necrosis [31, 37]. Hydrocephalus is present in 15 % of patients. On CT, SEGAs appear as hypo- to isodense lesions with variable degrees of calcification located near the foramen of Monro. On MRI, they are hypo- to isointense compared with cortex on T1-weighted and heterogeneously iso- to hyper-intense on T2-weighted images [37, 38] (Fig. 4a). Contrast enhancement is better seen on MRI than on CT [31].

White Matter Abnormalities

WM abnormalities include superficial abnormalities associated with cortical tubers, radial migration lines, and cyst-like WM lesions. On MRI, superficial WM abnormalities are seen as hyperintense areas on T2-weighted images and hypointense areas on T1-weighted images. Cyst-like WM lesions are located in the deep WM, typically near the lateral ventricles [31, 39]; they manifest on MRI as small well-demarcated lesions of similar intensity to the cerebrospinal fluid in all sequences [31]. Superficial WM abnormalities reflect reduced myelin or increased gliotic reaction, and cyst-like lesions seem to reflect cystic degeneration of WM or dilated perivascular spaces [31, 39].

Renal Manifestations

Renal Angiomyolipoma

AMLs are the most common mesenchymal renal neoplasms; they occur sporadically in 80 % of cases, most commonly in middle-aged women. The remainder of cases develop in association with TSC, seen in 70–80 % of these patients [40]. Compared with sporadic lesions, AMLs in TSC manifest at a younger age; tend to be multiple, larger, and bilateral; and are more prone to grow and require surgical resection [40]. AMLs are commonly incidental findings, but may manifest with abdominal pain, nausea, vomiting, and fever. Common clinical manifestations include a palpable mass, abdominal tenderness, hematuria, anemia, shock, hypertension, and renal failure. These signs and symptoms are usually the result of mass effect and hemorrhage. The most alarming complication of renal AMLs is rupture due to their abnormal vasculature, including aneurysm formation. The probability of rupture depends on the presence of aneurysm, which is related to the size of the AML [41]. On imaging, tumor size of 4 cm or larger and aneurysm size of 5 mm or larger were used as predictors of rupture with high sensitivity and specificity [41].

On ultrasound (US), AMLs appear as well-defined hyperechoic lesions [42]. CT allows the diagnosis by

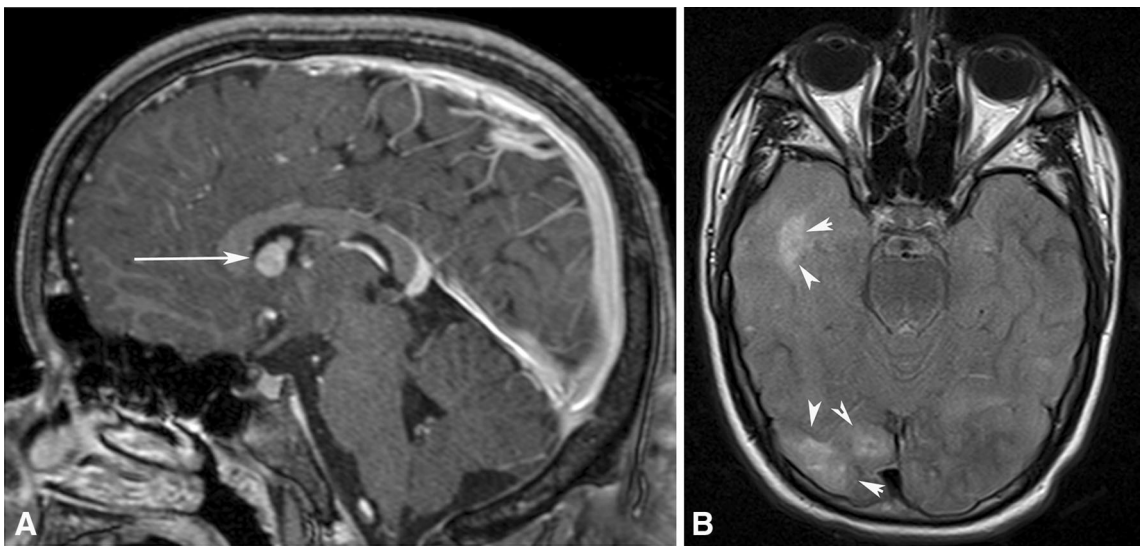

Fig. 4 A 13-year-old boy with tuberous sclerosis complex, intellectual disability, and tonic–clonic seizures. Post-contrast sagittal T1-weighted image (**a**) shows a nodule in the lateral ventricle close to the Monro foramina, suggesting giant cell subependymal astrocytoma (*arrow*). Axial FLAIR MRI (**b**) shows cortical tubers in the right temporal and occipital lobes as hyperintense areas (*arrowheads*)

demonstrating intratumoral macroscopic fat. CT attenuation measuring <–20 Hounsfield units on unenhanced images is characteristic [42] (Fig. 5). On MRI, AMLs with predominant fatty components are isointense relative to fat in all sequences [43]; signal intensity is typically higher than the renal parenchyma on T1-weighted images and homogeneous high signal intensity is typical on T2-weighted images. Demonstration of fat within the lesion when comparing images obtained before and after selective fat-suppression pulsing is most reliable [43]. The use of in-phase and out-of-phase imaging is also helpful. Notably, imaging features of AMLs, particularly lipid-poor lesions, and RCC overlap significantly [44].

Renal Cysts

Renal cysts or polycystic kidney disease may be seen in patients with TSC. As opposed to AMLs, renal cysts occur in young children [45]. Although generally asymptomatic, they can more frequently cause hypertension, renal failure, and retroperitoneal hemorrhage [11]. Typical US, CT, and MRI findings in TSC are bilateral multiple renal cysts in younger patients [11].

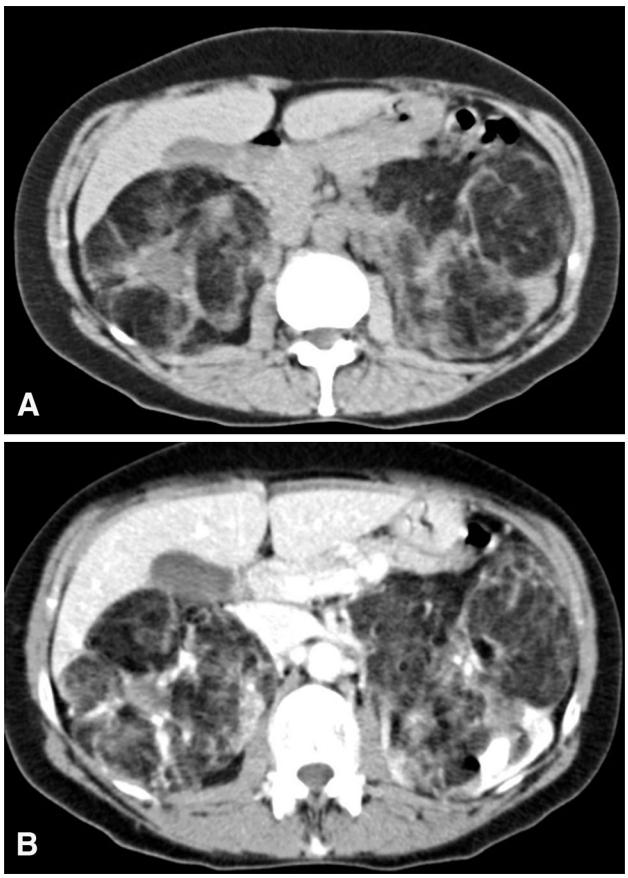

Fig. 5 A 53-year-old woman with tuberous sclerosis complex presenting with abdominal pain and palpable flank masses. Axial unenhanced (**a**) and contrast-enhanced (**b**) CT images demonstrate multiple fat-containing tumors in the kidneys, compatible with angiomyolipomas

Renal Cell Carcinoma

RCC is rare in TSC, with an estimated incidence of 2–4 %. This incidence is, however, higher than in the general population [46]. The average age of occurrence is 28 years, approximately 25 years earlier than in the general population [31]. In patients with TSC, RCC shows a striking female predominance, multifocality, and bilaterality [31]. A variety of cell types have been reported, including clear cell, papillary, and chromophobe carcinomas [47], and CT findings vary according to the subtype. Clear cell carcinoma, the most common subtype, is typically hypervascular on contrast-enhanced CT [46]; it is hypo- to isointense on T1-weighted and iso- to hyperintense on T2-weighted MRI [47]. The tumors may demonstrate considerable signal drop on out-of-phase MRI due to the presence of abundant fat [47]. Cystic changes are seen in up to 15 % and calcification in 10–15 % of these tumors [47, 48].

Dermatological Manifestations

Detection of characteristic skin lesions, which can appear anytime during childhood, is important in the diagnosis of TSC. The most common lesions are hypomelanotic macules, angiofibromas, shagreen patches, forehead plaques, and ungual fibromas [49]. Oral manifestations are frequent and characterized mainly by fibrous hyperplasia (angiofibromas) and dental pitting. Hypomelanotic macules, angiofibromas, ungual fibromas, shagreen patch, “confetti” skin lesions, and dental pits are part of the updated diagnostic criteria for TSC [50].

Hypopigmented macules have been described as the earliest visible sign of TSC [51]. They are typically round at one end and tapered at the other [49]. Approximately 90 % of patients with TSC have more than one hypomelanotic macule; 40 % have more than five nodules, which typically present within the first few years of life. The nodules remain stable for decades and become less apparent in late adulthood [49].

A distinct form of hypopigmentation consists of numerous small (1–2 mm) hypomelanic spots, called “confetti-like spots”, typically present in the limbs of 30 % of young children with TSC. These lighter patches of skin are caused by lack of melanin [45].

Facial angiofibromas (Fig. 6), formerly called adenoma sebaceum, are seen in approximately 75 % of patients with TSC [45]. They usually appear at 3–4 years of age, increase in number and size throughout the teenage years,

and become relatively stable during adulthood, typically appearing as small red papules in the malar area, with the so-called "butterfly distribution" [45].

Shagreen patch is an irregularly shaped, thickened and slightly elevated, soft skin-colored patch, usually seen on the lower back, formed by fibrous tissue. The name "shagreen" refers to a type of leather tanned to produce greenish knobs that resemble shark skin. This manifestation is characteristic of TSC and found in approximately 40 % of patients. It occurs in early childhood and may be the first sign of the disease [51].

Periungual fibromas (Koenen's tumors) are nodular lesions located around and under the toenails (90 %) or, less commonly, the fingernails (56 %). They are seen in approximately 20 % of patients, and are the last of the cutaneous lesions to appear, typically arising during adolescence or adulthood. Ungual fibromas are multiple in 75 % of cases [51].

Other Manifestations

Cardiac rhabdomyoma is a benign striated muscle tumor and the most common cardiac tumor in children (45 %) [52]. Approximately 75 % of these tumors occur before 1 year of age and may be seen before birth. Cardiac rhabdomyoma is common in TSC, with a reported frequency of 50–65 %; 40–80 % of patients with cardiac rhabdomyoma have TSC [31]. These tumors are seen in about 60 % of children, in contrast to 20 % of adults, with TSC, and this discrepancy is attributed to spontaneous tumor regression, particularly in the first 6 years of life [53]. Most rhabdomyomas are asymptomatic, with a minority causing arrhythmia and/or cardiac failure [53]. Echocardiography has been established as the primary diagnostic modality in children; on this modality, cardiac rhabdomyomas appear as multiple (or, less often, single) nodular lesions that are hyperechoic, well defined, and oval [52]. MRI can provide additional information regarding tumor extension and size, particularly in older patients and when echocardiography is suboptimal [54].

Fig. 6 A 13-year-old boy with tuberous sclerosis complex and multiple angiofibromas over the centrofacial area

Retroperitoneal LAM is histologically identical to its pulmonary counterpart and occurs in up to 20 % of patients with TSC–LAM [20]. Clinically significant disease is rare. Symptoms include abdominal bloating or discomfort, lymphedema and paresthesia of the lower extremities. On imaging, thick- or thin-walled cystic lesions can be found in the retroperitoneum, reflecting dilatation of lymphatic vessels due to obstruction. Enlarged lymph nodes, dilatation of the thoracic duct, ascites, and pleural effusion can be seen in retroperitoneal LAM [20, 31].

Skeletal abnormalities include cyst-like lesions, hyperostosis of the inner table of the calvaria, osteosclerotic changes, new periosteal bone formation, cystic changes in the phalanges, and scoliosis [55]. Cyst-like lesions are usually irregularly circumscribed and have sclerotic halos. Skull abnormalities consist of patchy areas of increased bone attenuation in the calvaria, generally occurring after puberty, most commonly in the parietal region. These changes have been shown to be due to hyperostosis of the inner table and of the trabeculae of the diploic spaces [55]. Spinal tumors have been reported very rarely in patients with TSC and are represented mainly by sacrococcygeal and cervical chordomas [56].

A variety of hepatobiliary lesions, including hepatomegaly, AMLs, lipomas, hamartomas, and fibromas, have been described in TSC. Most hepatic AMLs are sporadic. The incidence of hepatic AML in TSC (13 %) is much lower than that of AML in the kidney [57]. These lesions are typically small and multiple and show imaging features consistent with fat on US, CT, and MRI. They are, however, rarely hypoechoic on US, probably because of the small amounts of intratumoral fat. Variable enhancement is seen after contrast administration on CT and MRI. Chemical shift (in-phase and out-of-phase) MRI can be used to show the fat content of hepatic AMLs [58].

Conclusion

TSC is one of the most common multisystem neurocutaneous syndromes. It may present with various phenotypes and a wide variety of clinical and imaging manifestations. TSC should be suspected in the presence of classic lesions, such as cortical tubers, subependymal nodules, and WM abnormalities in the brain, cardiac rhabdomyoma, renal AML, skin lesions, and pulmonary LAM, even in the absence of suspicious clinical findings. Recognition of

various clinical and imaging features of TSC is pivotal in making a presumptive diagnosis, as well as defining the extent of the disease; it also aids decision making about disease management.

Conflict of interest None.

References

1. Syrbe S, Eberle K, Strenge S, Bernhard MK, Herbertz S, Bierbach U, Hirsch W, Froster UG, Kiess W, Merkenschlager A (2007) Neurofibromatosis type 1 and associated clinical abnormalities in 27 children. Klin Padiatr 219:326–332
2. Curatolo P (1996) Neurological manifestations of tuberous sclerosis complex. Childs Nerv Syst 12:515–521
3. Jansen FE, Vincken KL, Algra A, Anbeek P, Braams O, Nellist M, Zonnenberg BA, Jennekens-Schinkel A, van den Ouweland A, Halley D, van Huffelen AC, van Nieuwenhuizen O (2008) Cognitive impairment in tuberous sclerosis complex is a multifactorial condition. Neurology 70:916–923
4. Vogt H (1908) Zur pathologie und pathologischen anatomie der versclriedenen idiotieform. Mschr Psychiat Neurol 24:106–117
5. Shepherd CW, Gomez MR, Lie JT, Crowson CS (1991) Causes of death in patients with tuberous sclerosis. Mayo Clin Proc 66:792–796
6. Monteiro T, Garrido C, Pina S, Chorao R, Carrilho I, Figueiroa S, Santos M, Temudo T (2014) Tuberous sclerosis: clinical characteristics and their relationship to genotype/phenotype. An Pediatr (Barc) 81(5):289–296
7. Curatolo P, Bombardieri R, Jozwiak S (2008) Tuberous sclerosis. Lancet 372:657–668
8. Rok P, Kasprzyk-Obara J, Domanska-Pakiela D, Jozwiak S (2005) Clinical symptoms of tuberous sclerosis complex in patients with an identical TSC2 mutation. Med Sci Monit 11:230–234
9. Northrup H, Krueger DA, International Tuberous Sclerosis Complex Consensus Group (2013) Tuberous sclerosis complex diagnostic criteria update: recommendations of the 2012 international tuberous sclerosis complex consensus conference. Pediatr Neurol 49:243–254
10. Au KS, Northrup H (2010) Genotype-phenotype studies in TSC and molecular diagnostics. In: Kwiatkowski DJ, Whittemore VH, Thiele EA (eds) Tuberous sclerosis complex: genes, clinical features, and therapeutics. Wiley, Germany, pp 61–84
11. Crino PB, Nathanson KL, Henske EP (2006) The tuberous sclerosis complex. N Engl J Med 355:1345–1356
12. Franz DN, Brody A, Meyer C, Leonard J, Chuck G, Dabora S, Sethuraman G, Colby TV, Kwiatkowski DJ, McCormack FX (2001) Mutational and radiographic analysis of pulmonary disease consistent with lymphangioleiomyomatosis and micronodular pneumocyte hyperplasia in women with tuberous sclerosis. Am J Respir Crit Care Med 164:661–668
13. Johnson SR, Cordier JF, Lazor R, Cottin V, Costabel U, Harari S, Reynaud-Gaubert M, Boehler A, Brauner M, Popper H, Bonetti F, Kingswood C, Review Panel of the ERSLAMTF (2010) European Respiratory Society guidelines for the diagnosis and management of lymphangioleiomyomatosis. Eur Respir J 35:14–26
14. Taylor JR, Ryu J, Colby TV, Raffin TA (1990) Lymphangioleiomyomatosis: clinical course in 32 patients. N Engl J Med 323:1254–1260
15. Xu KF, Lo BH (2014) Lymphangioleiomyomatosis: differential diagnosis and optimal management. Ther Clin Risk Manag 10:691–700
16. Vianna FG, Marchiori E, Zanetti G, Mano CM, Sarcinelli-Luz B, Carvalho JF, Assed C, Santos IG, Santos AA, Vianna AD (2009) Tuberous sclerosis with pulmonary lymphangioleiomyomatosis and renal angiomyolipomas. Computed tomographic findings: a case report. Cases J 2:9238
17. Urban T, Lazor R, Lacronique J, Murris M, Labrune S, Valeyre D, Cordier JF (1999) Pulmonarylymphangioleiomyomatosis: a study of 69 patients. Groupe d'Etudes et de Recherchesurles Maladies "Orphelines" Pulmonaires (GERM"O"P). Med (Baltimore) 78:321–337
18. Oprescu N, McCormack FX, Byrnes S, Kinder BW (2013) Clinical predictors of mortality and cause of death in lymphangioleiomyomatosis: a population-based registry. Lung 191:35–42
19. Koo HK, Yoo CG (2013) Multiple cystic lung disease. Tuberc Respir Dis (Seoul) 74(3):97–103
20. Pallisa E, Sanz P, Roman A, Majo J, Andreu J, Caceres J (2002) Lymphangioleiomyomatosis: pulmonary and abdominal findings with pathologic correlation. Radiographics 22:S185–S198
21. Ryu JH, Doerr CH, Fisher SD, Olson EJ, Sahn SA (2003) Chylothorax in lymphangioleiomyomatosis. Chest 123:623–627
22. McCormack FX, Travis WD, Colby TV, Henske EP, Moss J (2012) Lymphangioleiomyomatosis: calling it what it is: a low-grade, destructive, metastasizing neoplasm. Am J Respir Crit Care Med 186:1210–1212
23. Travis WD, Brambilla E, Müller-Hermelink HK, Harris CC (2004) World Health Organization. World Health Organization Classification of Tumors. Pathology and Genetics. Tumours of the Lung, Pleura, Thymus and Heart. IARC Press. http://www.iarc.fr/en/publications/pdfs-online/pat-gen/bb10/BB10.pdf. Accessed 05 Feb 2015
24. Ryu JH, Tian X, Baqir M, Xu K (2013) Diffuse cystic lung diseases. Front Med 7:316–327
25. Dal Sasso AA, Belem LC, Zanetti G, Souza CA, Escuissato DL, Irion KL, Guimaraes MD, Marchiori E (2015) Birt-Hogg-Dubé syndrome. State-of-the-art review with emphasis on pulmonary involvement. Respir Med 109:289–296
26. Escuissato DL, de Almeida Teixeira BC, Warszwiak D, Zanetti G, Marchiori E (2014) Renal tumor associated with pulmonary cysts: Birt-Hogg-Dube syndrome. Q J Med 107(10):851–852
27. Marchiori E, Zanetti G, Hochhegger B, Irion KL (2012) Cystic amyloidosis or lymphoid interstitial pneumonia associated with amyloidosis? A diagnostic challenge. Ann Thorac Surg 94(3):1041–1042
28. Ray A, Paul S, Chattopadhyay E, Kundu S, Roy B (2015) Genetic analysis of familial spontaneous pneumothorax in an Indian family. Lung. doi:10.1007/s00408-015-9723-9
29. Muzykewicz DA, Black ME, Muse V, Numis AL, Rajagopal J, Thiele EA, Sharma A (2012) Multifocal micronodular pneumocyte hyperplasia: computed tomographic appearance and follow-up in tuberous sclerosis complex. J Comput Assist Tomogr 36:518–522
30. Muir TE, Leslie KO, Popper H, Kitaichi M, Gagne E, Emelin JK, Vinters HV, Colby TV (1998) Micronodular pneumocyte hyperplasia. Am J Surg Pathol 22:465–472
31. Umeoka S, Koyama T, Miki Y, Akai M, Tsutsui K, Togashi K (2008) Pictorial review of tuberous sclerosis in various organs. Radiographics 28:e32
32. Gomez MR (1988) Neurologic and psychiatric features. In: Gomez MR (ed) Tuberous sclerosis. Raven Press, New York, pp 21–36
33. Mizuguchi M, Takashima S (2001) Neuropathology of tuberous sclerosis. Brain Dev 23:508–515
34. DiPaolo D, Zimmerman RA (1995) Solitary cortical tubers. AJNR Am J Neuroradiol 16:1360–1364
35. Evans JC, Curtis J (2000) The radiological appearances of tuberous sclerosis. Br J Radiol 73:91–98

36. Zhou J, Shrikhande G, Xu J, McKay RM, Burns DK, Johnson JE, Parada LF (2011) Tsc1 mutant neural stem/progenitor cells exhibit migration deficits and give rise to subependymal lesions in the lateral ventricle. Genes Dev 25:1595–1600
37. Morimoto K, Mogami H (1986) Sequential CT study of subependymal giant-cell astrocytoma associated with tuberous sclerosis. Case report. J Neurosurg 65:874–877
38. Carvalho-Neto A, Bruck I, Antoniuk SA, Marchiori E, Gasparetto EL (2008) Proton MR spectroscopy of the foramen of Monro region in patients with tuberous sclerosis complex. Arq Neuropsiquiatr 66:303–307
39. Van Tassel P, Cure JK, Holden KR (1997) Cystlike white matter lesions in tuberous sclerosis. AJNR Am J Neuroradiol 18:1367–1373
40. Casper KA, Donnelly LF, Chen B, Bissler JJ (2002) Tuberous sclerosis complex: renal imaging findings. Radiology 225:451–456
41. Yamakado K, Tanaka N, Nakagawa T, Kobayashi S, Yanagawa M, Takeda K (2002) Renal angiomyolipoma: relationships between tumor size, aneurysm formation, and rupture. Radiology 225:78–82
42. Hélénon O, Merran S, Paraf F, Melki P, Correas JM, Chretien Y, Moreau JF (1997) Unusual fat containing tumors of the kidney: a diagnostic dilemma. RadioGraphics 17:129–144
43. Rofsky NM, Bosniak MA (1997) MR imaging in the evaluation of small (<or = 3.0 cm) renal masses. Magn Reson Imaging Clin N Am 5:67–81
44. Schieda N, Avruch L, Flood TA (2014) Small (<1 cm) incidental echogenic renal cortical nodules: chemical shift MRI out performs CT for confirmatory diagnosis of angiomyolipoma (AML). Insights Imaging 5:295–299
45. Leung AK, Robson WL (2007) Tuberous sclerosis complex: a review. J Pediatr Health Care 21:108–114
46. Ljungberg B, Campbell SC, Choi HY, Jacqmin D, Lee JE, Weikert S, Kiemeney LA (2011) The epidemiology of renal cell carcinoma. Eur Urol 60:615–621
47. Prasad SR, Humphrey PA, Catena JR, Narra VR, Srigley JR, Cortez AD, Dalrymple NC, Chintapalli KN (2006) Common and uncommon histologic subtypes of renal cell carcinoma: imaging spectrum with pathologic correlation. Radiographics 26:1795–1806 **(discussion 1806–1810)**
48. Jinzaki M, Tanimoto A, Mukai M, Ikeda E, Kobayashi S, Yuasa Y, Narimatsu Y, Murai M (2000) Double phase helical CT of small renal parenchymal neoplasms: correlation with pathologic findings and tumor angiogenesis. J Comput Assist Tomogr 24:835–842
49. Teng JM, Cowen EW, Wataya-Kaneda M, Gosnell ES, Witman PM, Hebert AA, Mlynarczyk G, Soltani K, Darling TN (2014) Dermatologic and dental aspects of the 2012 international tuberous sclerosis complex consensus statements. JAMA Dermatol 150:1095–1101
50. Torrelo A, Hadj-Rabia S, Colmenero I, Piston R, Sybert VP, Hilari-Carbonell H, Hernandez-Martin A, Ferreres JC, Vano-Galvan S, Azorin D, de Salamanca JE, Requena L, Bodemer C, Happle R, Garcia-Patos V, Fraitag S (2012) Folliculocystic and collagen hamartoma of tuberous sclerosis complex. J Am Acad Dermatol 66:617–621
51. Webb DW, Clarke A, Fryer A, Osborne JP (1996) The cutaneous features of tuberous sclerosis: a population study. Br J Dermatol 135:1–5
52. Uzun O, Wilson DG, Vujanic GM, Parsons JM, De Giovanni JV (2007) Cardiac tumours in children. Orphanet J Rare Dis 2:11
53. Kotulska K, Larysz-Brysz M, Grajkowska W, Jozwiak J, Wlodarski P, Sahin M, Lewin-Kowalik J, Domanska-Pakiela D, Jozwiak S (2009) Cardiac rhabdomyomas in tuberous sclerosis complex show apoptosis regulation and mTOR pathway abnormalities. Pediatr Dev Pathol 12:89–95
54. Matsumura M, Nishioka K, Yamashita K, Yoshibayashi M, Okuno T, Konishi J, Shimizu T, Temma S, Ueda T, Mikawa H (1991) Evaluation of cardiac tumors in tuberous sclerosis by magnetic resonance imaging. Am J Cardiol 68:281–283
55. Holt JF, Dickerson WW (1952) The osseous lesions of tuberous sclerosis. Radiology 58:1–8
56. Lee-Jones L, Aligianis I, Davies PA, Puga A, Farndon PA, Stemmer-Rachamimov A, Ramesh V, Sampson JR (2004) Sacrococcygeal chordomas in patients with tuberous sclerosis complex show somatic loss of TSC1 or TSC2. Genes Chromosom Cancer 41:80–85
57. Fricke BL, Donnelly LF, Casper KA, Bissler JJ (2004) Frequency and imaging appearance of hepatic angiomyolipomas in pediatric and adult patients with tuberous sclerosis. AJR Am J Roentgenol 182:1027–1030
58. Balci NC, Akinci A, Akun E, Tunaci A (2002) Hepatic angiomyolipoma: demonstration by out of phase MRI. Clin Imaging 26:418–420